A Relation between the T/S Curve and the ratio of Oceanic to Atmospheric Poleward Heat Transport in Middle Latitudes

Christopher Dancel *

Dept. of Physics, Imperial College, Prince Consort Road, London, SW7 2AZ, United Kingdom

Arnaud Czaja

Dept. of Physics, Imperial College, Prince Consort Road, London, SW7 2AZ, United Kingdom

* *Corresponding author address:* Christopher Dancel, Dept. of Physics, Imperial College, Prince Consort Road, London, SW7 2AZ, United Kingdom

E-mail: christopher.dancel04@imperial.ac.uk

ABSTRACT

We build on the work of Stommel and Csanady (1980) who showed that the ratio of oceanic transport of heat H_o and freshwater F is a simple function of hydrographic properties. By explicitely relating F to the atmospheric poleward transport of heat (H_a) in midlatitudes, we are able to derive a simple formula for the ratio of ocean to atmosphere poleward heat transport,

$$\frac{H_o}{H_a} \approx \frac{c_o S_o}{l_v} \frac{\mu}{1+\gamma}$$

In this relation, S_o is the global mean ocean salinity, c_o is the specific heat capacity of sea water, l_v is the enthalpy of vaporisation of water, γ is the ratio of dry static energy to latent heat transport in the atmosphere, and μ is the temperature - salinity slope drawn by meridionally moving waters. Interestingly, the ratio H_o/H_a in the above relation does not explicitely depend on the intensity of oceanic and atmospheric mass transports.

In this paper we show the validity of this relation using a combination of observations and outputs from a global climate model.

1. Introduction

Estimates of oceanic and atmospheric poleward heat transport have been published over the years, yet there is generally little agreement over the order of magnitude of the contribution of the ocean and the atmosphere to the total poleward energy transport in middle latitudes. In the 70s, estimates by Vonder Haart and Oort (1973) suggested a comparable amplitude for oceanic (H_o) and atmospheric (H_a) northward heat transport at $40°N$

($H_o \approx H_a \approx 2PW$). This was later confirmed by the analysis of Carissimo et al. (1985), who extended this result to extra-tropical latitudes of the Southern Hemisphere. More recently, however, Trenberth and Caron (2001) produced estimates with a much larger contribution of the atmosphere to the total poleward heat transport than the ocean in middle latitudes (for latitudes poleward of 30°). Interestingly, the dominance of the atmosphere in middle latitudes suggested by Trenberth and Caron (2001) was hinted at in much earlier studies, for instance, in Bjerknes' monograph on Atlantic air-sea interactions (1964), using data from Houghton (1954) and Sverdrup (1957).

On the observational side, it is clear that there are serious issues regarding uncertainties in each of the above estimates of H_o and H_a (e.g., Wunsch, 2005). On the theoretical side, the question of why should the atmosphere or the ocean dominate the total poleward heat transport in middle latitudes or elsewhere is still open despite recent attempts at addressing this problem (Held, 2001; Czaja and Marshall, 2006). Middle latitudes are particularly resistant to simple explanations because of the difficulty in parameterizing the heat transport by atmospheric baroclinic waves and oceanic eddies, and because of the lack of a simple theoretical framework to predict the heat transport of the large-scale ocean circulation beyond that associated with Sverdrupian (horizontal) gyres.

In this study, we bypass these difficulties by using an earlier result on the ratio of ocean heat to freshwater transport due to Stommel and Csanady (1980). From simple arguments these authors showed that this ratio solely depends on the mean salinity of the oceans and the slope of the oceanic temperature/salinity relationship. Acknowledging that the oceanic freshwater transport is proportional to the atmospheric latent heat transport, itself a major contributor atmospheric heat transport in middle latitudes (e.g., Pierrehumbert,

2002), we obtain a simple expression for the ratio H_o/H_a. The latter is found typically smaller than unity, suggesting, from fairly general and robust arguments, a dominant role for the atmosphere in transporting heat poleward in middle latitudes.

The paper is structured as follows. Section 2 describes Stommel and Csanady's analysis. Section 3 rephrases the latter into the problem at hand, and derives the above mentioned formula for the ratio H_o/H_a. In Section 4 we test the formula against outputs from the Hadley Centre HadCM3 coupled climate model while, in section 5, we test it against hydrographic observations taken during the World ocean Circulation Experiment (WOCE). Discussion and conclusions are offered in section 6 and 7, respectively.

2. Stommel and Csanady's analysis

We denote by M and F the total amount of oceanic water mass and atmospheric water mass moving poleward across a given latitude circle per unit time, respectively (Fig. 1). Conservation of mass requires that, in the long term, the total mass of ocean waters moving equatorward per unit time be $M+F$. If T denotes the (mass weighted) averaged temperature of these oceanic water masses, and $T+\Delta T$ the (mass weighted) temperature of the oceanic water masses going poleward, the oceanic heat transport H_o across the latitude circle is then,

$$H_o = c_o M\,(T+\Delta T) - c_o\,(M+F)\,T \tag{1}$$

in which c_o is the specific heat capacity of seawater. Conversely, the steady state salt budget for the portion of ocean poleward of the given latitude circle reads,

$$0 = M\,(S+\Delta S) - (M+F)\,S \tag{2}$$

in which S and $S + \Delta S$ denote the (mass weighted) averaged salinity of the oceanic water masses going equatorward and poleward, respectively. A simple but powerful deduction from (2) is that in order to accommodate for the poleward atmospheric transport of moisture ($F > 0$), seawater moving poleward must be saltier ($\Delta S > 0$) than that moving equatorward.

The meridional mass transport of water in the ocean is much larger than that in the atmosphere, $M \gg F$. Indeed, using (2) we obtain,

$$M = F\frac{S}{\Delta S} \tag{3}$$

so that, using typical numbers $F = 1\ Sv$ ($1Sv = 10^6 m^3/s$), $S = 35psu$, and $\Delta S = 1psu$, Eq. (3) yields $M = 35Sv$ (as we shall see later, values of M can be even much larger than this). This allows to simplify (1) into

$$H_o \approx c_o M \Delta T \tag{4}$$

Using (4) and (3), and approximating the salinity of equatorward moving waters by the mean ocean salinity S_o, i.e., $S \simeq S_o$, we readily obtain

$$\frac{H_o}{F} \approx c_o S_o \frac{\Delta T}{\Delta S} \tag{5}$$

Stommel and Csanady (1980) used eq. (5) to test the accuracy of indirect estimates of oceanic heat and freshwater transports from radiative measurements and direct calculations of atmospheric water vapour transports from radiosondes, arguing that the r.h.s of (5) can be computed from hydrographic sections. Below we use this relation to estimate the partitioning of poleward heat transport between ocean and atmosphere.

A few qualitative remarks apply before doing so. Since moisture is transported poleward in the atmosphere in midlatitudes ($F > 0$), a poleward oceanic heat transport ($H_o > 0$)

requires from (5) that the slope of the T/S curve be positive. This is typically the case in the North Atlantic where warm and salty waters are transported poleward in the upper layer of the column and colder and fresher waters are transported southward at depth. Conversely, an equatorward oceanic heat transport, as occurs in the South Atlantic (e.g., Bryden and Isawaki, 2001), requires from (5) that the T/S slope be negative. This is consistent with the presence of a salinity minimum (change of sign of the slope in the T/S curve) associated with Antarctic Intermediate Water in the Southern Ocean.

3. Oceanic to atmospheric heat transport ratio

a. Derivation of a simple expression for the ratio H_o/H_a

The energy per unit mass carried by an air parcel is, neglecting the small contribution from kinetic energy, the moist static energy h (Neelin and Held, 1987),

$$h = c_p T_a + \Phi + l_v q \tag{6}$$

In (6), c_p and l_v are the specific heat capacity of dry air and enthalpy of vaporization of water, respectively, T_a is air temperature, q specific humidity and Φ is gravitational potential energy per unit mass. The relative contribution of dry static energy ($c_p T_a + \Phi$) and latent heat ($l_v q$) to the meridional transport of moist static energy is measured by the parameter γ,

$$\gamma \equiv \frac{c_p \overline{v T_a} + \overline{v\Phi}}{l_v \overline{vq}} \tag{7}$$

in which v is the meridional velocity of air and an overbar denotes an average along a latitude circle.

In the extra-tropical atmosphere, the dominant mechanism of energy transport across a latitude circle is through deviations from the zonal mean, i.e., eddies (e.g., Oort and Peixoto, 1992). The meridional moist static energy transport at a given pressure level is then,

$$\overline{vh} \approx \overline{v'h'} = c_p\overline{v'T_a'} + \overline{v'\Phi'} + l_v\overline{v'q'} \tag{8}$$

in which primes denote deviations from the zonal average. Since atmospheric eddies are to leading order in geostrophic balance,

$$v' \approx \frac{1}{f}\frac{\partial \Phi'}{\partial x} \tag{9}$$

f denoting the Coriolis parameter and x the distance in the east-west direction, there is no net transport of potential energy across a latitude circle, $\overline{v'\Phi'} \propto \overline{\Phi'\partial\Phi'/\partial x} = 0$. Equation (8) and (7) can thus be further simplified into,

$$\overline{vh} \approx c_p\overline{v'T_a'} + l_v\overline{v'q'} \tag{10}$$

and

$$\gamma \approx \frac{c_p\overline{v'T_a'} + \overline{v'\Phi'}}{l_v\overline{v'q'}} \approx \frac{c_p\overline{v'T_a}}{l_v\overline{v'q'}} \tag{11}$$

Integrating (10) in the vertical, the total atmospheric energy (or simply heat) transport across a given meridional section reads,

$$H_a = \int \overline{vh}\frac{dp}{g} \approx \int (1+\gamma)\overline{v'q'}\frac{dp}{g} \tag{12}$$

Within a midlatitude baroclinic wave (storm), temperature and specific humidity perturbations are correlated, as the wave moves warm/moist air poleward and upward and dry/cold air equatorward and downward. The two terms on the r.h.s of (10) are thus two faces of the

same process, both transporting energy poleward. Typically the contribution of temperature and moisture transports are comparable, since, using typical values of temperature and specific humidity perturbations within a storm (5-10K and 5-10g/kg, respectively), the ratio $\gamma \approx 1$.

At leading order in the extra-tropics, H_a can thus simply be estimated from (12) as

$$H_a \approx (1+\gamma)\, l_v F \tag{13}$$

in which we have further used

$$F = \int \overline{vq}\frac{dp}{g} \simeq \int \overline{v'q'}\frac{dp}{g} \tag{14}$$

to keep consistency with (8). Note that equation (13) would be a very poor approximation of the atmospheric energy transport in the Tropics, since it is primarily potential energy which is transported poleward, sensible ($c_p T_a$) and latent energy ($l_v q$) being transported equatorward by the mean meridional (Hadley) circulation.

Combination of (13) and (5) provides the relation for the ratio of oceanic to atmospheric poleward heat transport across a given midlatitude circle,

$$\frac{H_o}{H_a} \approx \frac{c_o}{(1+\gamma)\, l_v} S_o \frac{\Delta T}{\Delta S} \tag{15}$$

By introducing

$$\mu \equiv \frac{\Delta T}{\Delta S} \tag{16}$$

we can rewrite (15) as

$$\frac{H_o}{H_a} \approx \frac{c_o S_o}{l_v} \frac{\mu}{1+\gamma} \tag{17}$$

The ratio is seen to depend solely upon thermodynamics constants (specific heat capacity and enthalpy of vaporization), the mean ocean salinity, the slope μ of the T/S curve drawn by the

water masses moving poleward and equatorward, and the ratio γ of atmospheric dry static energy to latent heat transport. Only geostrophy and the hypothesis that eddies dominate atmospheric transports have been assumed. Considering the complexity of the fluid motions and diabatic processes associated with oceanic and atmospheric heat transports, relation (17) is a powerful and simple relation to compute their ratio.

b. Physical interpretation

One interesting aspect of the relation (17) is that it does not involve the ratio of oceanic to atmospheric mass transport, although the latter has been shown to be crucial in setting the partioning of heat transport in midlatitudes (Czaja and Marshall, 2006). To see how this can be, we consider the limit in which the atmospheric heat transport is dominated by the transport of latent heat, $H_a \simeq l_v F$ (i.e., $\gamma \to 0$). In this limit, the atmospheric heat transport is achieved by transporting meridionally air masses of different moisture content (Δq), the associated mass transport M_a being set by the intensity and scale of the baroclinic waves. We can thus write,

$$\frac{H_o}{H_a} \simeq \frac{H_o}{l_v F} = \frac{H_o}{M_a l_v \Delta q} = \frac{M}{M_a} \frac{c_o \Delta T}{l_v \Delta q} \tag{18}$$

A comparison of this expression with (15) when $\gamma = 0$ shows then that,

$$\frac{\Delta S}{S_o} = \Delta q \frac{M_a}{M} \tag{19}$$

This equation makes it clear that the information on the ratio of mass transports is indeed implicit in the oceanic salinity contrast. This arises because, salt not being exchanged at the air-sea interface, the salinity of water moving poleward must be greater than that going

equatorward in order to accomodate for the poleward atmospheric transport of water vapour F –Eq. (2). Since F is proportional to M_a, the salinity balance in effect couples M and M_a. Note that there is nothing special about salt here: a similar constraint on the ratio M/M_a would be found for any other tracer not having surface or interior sources and sinks.

4. Test of the Relationship in a Coupled Climate Model

a. Heat Transport and Partitioning in HadCM3

The validity of (17) was tested using the Hadley Centre HadCM3 coupled climate model (Cox et al. 1999; Gordon et al. 2000; Pope et al. 2000). We used the years 640 - 650 from spin-up of the control run simulation to calculate a monthly mean climatology for all model calculations. The ocean model setup comprised of a 1.25° by 1.25° horizontal resolution with 20 vertical layers, whilst the atmospheric model has a resolution of 3.75° longitude by 2.5° latitude with 19 vertical layers.

The oceanic heat transport H_o was calculated from the horizontal divergence of surface flux at the ocean-atmosphere interface (we removed ocean heat storage by subtracting the small temporal and spatial mean surface flux value, $0.02 W m^{-2}$, from the incoming surface flux); we name this version of heat transport, H_o^{true}, where the 'true' superscript corresponds to the total ocean heat transport (Fig. 2, solid). The ocean heat transport was also computed using (4), which we name H_o^{reso} (Fig. 2, dotted), where the 'reso' superscript indicates that this method is only measuring the resolved advective component of the heat transport (see next subsection for details on M and ΔT)

Due to the coarseness of the ocean horizontal resolution, subgrid-scale processes eg. meso-scale eddies and diffusive effects, are indirectly measured as the difference between H_o^{true} and H_o^{reso} in Fig. 2. The implied eddy heat transport within northern hemisphere extra-tropical latitudes are almost neglible, whereas it is comparable to H_o^{res} for the southern hemisphere. The direction of parameterised eddy heat transport is consistent with ocean eddies transporting heat equatorward at low latitudes and poleward at high latitudes (e.g. Jayne and Marotzke, 2002).

Both methods of calculating ocean heat transport illustrates an antisymmetric distribution about the equator, with the northern hemisphere transporting almost twice as much heat within the tropical regions (peak magnitude of $1.7PW$ at $15°N$) as compared to its southern hemisphere counterpart. The larger northern hemisphere heat transport stems mostly from the Atlantic basin in which the Southern Altantic Ocean advects heat *northwards*, opposing the other basins' poleward heat transport, as discussed previously (section 2).

To compute the atmospheric heat transport H_a (Fig. 2, black dashed) we use the same method as Wunsch (2005) who indirectly measured the latter as the difference between total heat transport (not shown) and H_o^{true}. The total heat transport was calculated using the same methodology used for H_o^{true}, i.e., after removing the small temporal and spatial mean net flux value of $-0.06Wm^{-2}$ at the top of the atmosphere. As found for the ocean heat transport, the distribution of H_a is antisymmetric about the equator, with peak magnitudes $4.6PW$ at $37.5°N$, and $-4.7PW$ at $40°S$. Within the deep tropics, the atmosphere transports very little heat energy polewards due to the almost near cancellation of latent and dry static energy within the tropical Hadley Cells. The ocean therefore is the main carrier of heat

within the tropics. The atmospheric role to transport heat becomes increasingly important the further poleward, with baroclinic instabilities at mid-latitudes being the main driver. The atmosphere is therefore the main carrier of heat for extra-tropical latitudes.

b. Calculations of M, F, ΔT, ΔS, and μ

Calculations of M, F, ΔT and ΔS were carried out using the model outputs of meridional velocity V, T and S. The latter variables were interpolated onto a regular fine (ΔZ=10m) vertical grid. The vertical resolution of 10m thickness was chosen to accurately represent the layers closest to the ocean surface. Mass conservation was enforced across a latitude circle by subtracting from V its average value over the section. For each latitude we plotted meridional mass transport as a function of temperature and salinity bins, $M(T, S)$, using

$$M(T,S) = \frac{1}{\delta T \delta S} \int_0^{L_x} \int_{-H}^{0} \int_{T}^{T+\delta T} \int_{S}^{S+\delta S} \rho_o v dx dz dT' dS' \tag{20}$$

where $\rho_o = 1025 kgm^{-3}$ is a reference ocean density, H represents ocean depth, L_x is the length of the given latitude circle, and temperature and salinity resolution is set $\delta T = 0.2°C$ and $\delta S = 0.1 psu$ respectively. Fig. 3 shows the resulting mass transport at $40°N$. One distinguishes clearly between the warm and salty water masses found within the North Atlantic ($S > 35 psu$), and the relatively cool and fresher water masses within the North Pacific ($S < 35 psu$). To compute poleward flowing mass weighted values of temperature T_p and salinity S_p, we find the 'centre of mass' point for poleward flowing waters on the $M(T, S)$ plot (dark shaded bins), whose coordinates correspond to T_p and S_p. As an example, for Fig. 3 the centre of mass point for poleward flowing waters is centered at $34.7 psu$ and

$6.3°C$ (intersection between horizontal black solid and vertical black dashed line), therefore at $40°N$, $T_p = 6.3°C$ and $T_p = 34.7psu$. It is seen that this center of mass truly is an average over Atlantic and Pacific watermasses. To compute equatorward flowing mass weighted values, T_e and S_e, we follow the same methodology (white lines in Fig. 3), but instead compute the centre of mass point for all equatorward flowing values of $M(T, S)$ (light shaded bins in Fig. 3). From these values we readily obtain $(\Delta T, \Delta S) = (T_p, S_p) - (T_e, S_e)$.

The latitudinal distributions of these variables can be seen in Fig. 4, with ΔS and F being multiplied by a factor of 10 and 1000 respectively to magnify detail; black (grey) lines represents the Northern (Southern) Hemisphere. The latitudinal axis for the Southern Hemisphere is flipped to have a shared axis with Northern Hemisphere values.

Northern Hemisphere averaged ΔT is on the order of 2°C for the extra-tropics (Fig. 4a, black, solid). Although not shown the Atlantic basin has the largest temperature contrast of $\Delta T \approx 4°C$, with the Indo-Pacific basin having a combined $\Delta T \approx 1°C$. Similarly an average $\Delta S \approx 0.2psu$ (Fig. 4a, black, dashed) stems largely from the Atlantic basin with values of $\Delta S \approx 0.3psu$ and $\Delta S \approx 0.1psu$ for the Indo-Pacific region. This is consistent with the fact that the Atlantic basin is saltier and warmer than all others. For the Southern Hemisphere (grey curves), both quantites are reduced especially ΔT, with an average $\Delta T < 0.1$, and ΔS a factor 2 smaller than in the Northern Hemisphere. Southward of $64°S$ salinity increases with depth to a maximum of $\approx 35psu$ at 4500m. At these latitudes, the equatorward flow of waters originating within the Ross and Weddell Sea's extend almost to the bottom of the sea floor. These deep equatorial flowing waters pick up the high salinity values associated with depth, leading to a reversal in sign of ΔS at $64°S$.

Mass transports (here expressed in Sv by dividing by a constant density ρ_o) for the

northern hemisphere ranges between $200Sv$ at mid-latitudes to $20Sv$ at higher latitudes (Fig. 4b, black, solid). For the southern hemisphere, a peak in meridional mass transport of $700Sv$ is found at $57°S$. It should be emphasised that M represents the summation over *all* northward or *all* southward velocity cross sectional areas; this is to be contrasted with the standard Eulerian mean calculation which computes the net values of northward minus southward mass transport at every depth layer. The increase in meridional mass transport for the Southern Hemisphere region corresponds to there being a larger fraction of ocean area (this be equal to 100% ocean area for the Southern Ocean region). The Northern Hemisphere ocean heat transport, when compared to its Southern counterpart, differs therefore by its large temperature contrast and small mass transport.

The atmospheric freshwater fluxes F/Sv (Fig. 4b, dashed) were computed using (3) ie. $F = M\Delta S/S_o$. Both hemispheres have similar magnitudes near the Tropical boundaries, and display an almost complete reduction near polar latitudes. This decrease is particularly pronounced in the Southern Hemisphere, with cold Antarctic temperatures decreasing the saturation specific humidity of air. The Southern Hemisphere does however transport more than twice as much freshwater than the Northern Hemisphere poleward of $45°S$, possibly due to the greater presence of ocean surface and tropical rainforest regions (ie. the Amazon basin) for the former hemisphere.

The ratio $\mu \equiv \Delta T/\Delta S$ (Fig. 5a, black) is greater in the Northern than in the Southern Hemisphere, this being mainly due to the large temperature contrast ΔT, originating from the meridional overturning circulation found in the North Atlantic. The reduced values of μ for the southern hemisphere reflects the greater reduction in ΔT compared to ΔS. The sudden drop in μ at $64°S$ corresponds to where ΔS changes sign. It is interesting to note

that even though the observed ratio of H_o/H_a is similar for both hemispheres (anticipating slightly on Fig. 6), values of μ in each hemisphere vary by almost an order of magnitude at some latitudes. According to (17) the large fluctuations for the latter term must be partially balanced by changes in γ to balance out the heat transport ratio H_o/H_a (we come back to this issues in the discussion section).

c. Test of the Formula

Fig. 6 compares the model distribution of H_o/H_a (solid) with the predicted ratio (dashed) computed using (17) and using $\gamma = (H_a - l_v F)/l_v F$, where F is the freshwater transport shown in Fig. 5b; this expression will be referred to as γ_F. Northern Hemisphere H_o/H_a values (black) show a close agreement between predicted (dashed) and observed (solid) quantities. The minimum at $40°N$ coincides with the locations of the major western boundary currents e.g. the Gulf Stream and Kuroshio. These fast moving currents are warmer than their surroundings and therefore provide a source of heat for the atmosphere. These help fuel the mid-latitude storms that are blown eastward, while at the same time reducing the heat transport by the ocean. In a more "gyral" explanation, the separated western boundary currents transports most of its heat zonally, thus having a vanishing meridional component of velocity. Both explanations help explain the decrease in H_o and therefore a subsequent decrease in (17).

The ratio of ocean to atmosphere heat transport in HadCM3 is smaller in the Southern than in the Northern Hemisphere, being due to the smaller contribution of H_o at these latitudes by almost a factor of 2, whilst the atmospheric component increases to compensate,

leaving an almost perfect anti-symmetric distribution of total heat transport. Polewards of $40°S$ predicted values of (17) do not fit well with the true model values, owing to the large parameterized eddy component of heat transport within the southern hemisphere (Fig. 2, section 4a) which was not taken into account in the calculations of M, ΔT and ΔS.

d. Constraining the Theory even further

Equation (17) provides a good approximation to H_o/H_a using ΔT, ΔS and γ. In order to simplify (17) even further by using solely temperature and salinity as variables, a new expression for γ that is solely dependent on surface temperature T_s was developed. By setting a constant relative humidity RH, one can scale fluctuations in specific humidity q' to fluctuations in lower tropospheric air temperatures, analogous to warm (cold) air carrying more (less) moisture. Through invoking the Clausius-Clapeyron relationship and approximating lower tropospheric air temperature as similar to T_s, we compute a new expression for γ, hereafter denoted by γ_{T_s}

$$\gamma_{T_s} = \frac{c_p R}{l_v^2 RH} \frac{T_s^2}{q_{sat}\,(Ts)} \tag{21}$$

where $R = 287 Jkg^{-1}K^{-1}$ is the gas constant, $RH = 0.8$ is constant relative humidity, q_{sat} is the saturation specific humidity, and T_s is the zonal average surface temperature – the full derivation of this equation is given in the Appendix. The resulting heat transport ratio using this new function of γ_{T_s} is shown in Fig. 6 (dotted), displaying a comparable skill as when using γ_F.

5. Application to Oceanic Observations

Testing the relation (17) in observations might at first sight seem daunting, since it requires a knowledge of global, three dimensional meridional mass transports in order to estimate ΔT and ΔS. We propose here an alternative application of (17) to the Southern ocean using the assumption that in some latitude band, the ocean heat transport is dominated by its eddy component. Such assumption is reasonable near $45°S$ as recent high resolution ocean models have suggested (e.g., Jayne and Marotzke, 2002; Meijers et al., 2007).

Under the assumption that it is meso-scale eddies, rather than quasi-steady gyres or overturning cells, which are the major contributors to the ocean heat transport near $45°S$, the ratio $\Delta T/\Delta S$ associated with oceanic eddies can be estimated from lateral gradients in temperature and salinity. Let us denote by l the typical excursion of water parcels within an eddy in the (meridional) y direction. The temperature difference ΔT_{eddy} between equatorward and poleward flowing parcels is then

$$\Delta T_{eddy} = 2l \times \frac{\partial T}{\partial y} \tag{22}$$

Application of a similar reasoning to salinity contrasts ΔS_{eddy} yields a simple relation for the ratio $\Delta T/\Delta S$ appearing in (15),

$$\frac{\Delta T}{\Delta S} \approx \frac{\Delta T_{eddy}}{\Delta S_{eddy}} = \frac{\partial T}{\partial y} \Big/ \frac{\partial S}{\partial y} \tag{23}$$

To estimate the oceanic to atmospheric heat transport ratio at $45°S$, we thus need to estimate the ratio of temperature to salinity gradients over the layer in which eddy-induced lateral displacements are significant (0-1000m, e.g., Wunsch, 1999). In Fig. 7, we present a scatterplot of observed meridional temperature/salinity changes across the Sub-Antarctic Front at

$45°S/120°E$, estimated as $\Delta T_{eddy} \approx T(46°S) - T(45°S)$ and $\Delta S_{eddy} \approx S(46°S) - S(45°S)$, using the data taken during the World Ocean Circulation Experiment (WOCE, see White, 1994) with a roughly 0.5° resolution in latitude. The scatterplot is seen to be composed of three well separated regions, indicated by the black circles (0-600db), grey circles (600-700db) and black stars (700-1000db). Within the upper layer (black circles, including the mixed layer, seasonal thermocline and a well defined layer of subantarctic mode water), a sharp linear relation is found with a value $\mu \equiv \Delta T/\Delta S = 8K/psu$, over a broad range of temperature (0 to 2.5K) and salinity (0 to 0.3 psu) contrasts. The lower layer (black stars) shows a similar range of salinity contrasts but twice stronger temperature contrasts.

We further need an estimate of γ in order to predict the ratio H_o/H_a from (17). This is obtained from atmospheric reanalyses data with the results that, at $45°S$, $\gamma \simeq 2PW/2.6PW = 0.77$ (Pierrehumbert, 2002; by inspection of his Fig. 1a). Application of (17) at $45°S$ thus yields,

$$\frac{H_o}{H_a} \approx \frac{4000 \times 35}{2.5 \times 10^6} \times \frac{8}{1 + 0.77} \approx 0.25 \tag{24}$$

which is in agreement with a dominance of the atmospheric contribution to the total poleward heat transport in the Southern Hemisphere (e.g., Trenberth and Caron, 2002; Czaja and Marshall, 2006).

6. Discussion

Besides its domain of validity being restricted to midlatitudes, there are two main limitations of the formula (17) that we wish to discuss. First, it is based on the assumption that the

coupled ocean-atmosphere freshwater balance has reached equilibrium –see eq. (2). "Hosing experiments" in which the North Atlantic overturning circulation is artificially reduced (e.g., Stouffer et al., 2006) show that this might only be achieved on timescales of centuries. Our comparison of predicted and true ratio H_o/H_a for the northern hemispheric extra-tropical latitudes indicates discrepancies on the order of $10-20\%$, depending on the choice of γ (Fig. 6) used in (17). These errors originate from the the fact that the hydrological cycle has not completely reached equilibrium yet, i.e. that in practice that there are differences between the indirect calculation of atmospheric freshwater transport F using (3), and the direct calculation using evaporation minus precipitation (by inspection of Pardaens et al. 2003, Fig. 3).

Second, although the framework used to derive (17) allows ocean eddies to be included, it does so only partially. A rough observational estimate of the advective effects of the eddies was proposed in section 5 (and, in an ocean model framework, the "bolus" velocities associated with eddy parameterization could be used explicitely to calculate M and F), but it is impossible to include the diffusive effect of the eddies (e.g., Plumb and Mahlman, 1987) in a mass transport framework.

Inspection of the variables μ and γ (section 4b) revealed that their magnitudes are both larger for the Northern than for the Southern Hemisphere. Although the observed model ratio H_o/H_a is approximately twice as large within the Northern Hemisphere, μ and γ vary by almost a factor of 8 and 3 respectively when comparing hemispheres (e.g. at $40^\circ N, S$), suggesting a form of compensation between the two variables. A naive view to explain this compensation could be as follows: we rewrite our expression for the ratio of dry static energy to latent heat transport in the atmosphere γ, as $\gamma = (H_a - l_v M \frac{\Delta S}{S})/l_v M \frac{\Delta S}{S}$, where

dry static energy is computed as the residual between atmospheric and latent heat transport, and freshwater transport F is rewritten using (3). Since γ and the T/S slope $\mu = \frac{\Delta T}{\Delta S}$ thus appear inversely proportional to ΔS, this latter quantity would be a suitable candidate for the coupling between the two terms (given all other quantities remain unchanged). However if we compare ΔS for the Northern and Southern Hemispheres we find that ΔS is *larger* for the former region, giving smaller values for μ and γ; the opposite to what we would expect from a simple ΔS coupling. The actual reduction in μ for the Southern Hemisphere is thus primarily controlled by the reduction in ΔT. To explain the reduction in γ we showed from our previous expression of γ above, that γ is both inversely propertional to ΔS *and* meridional mass transport M. By inspection, differences between each hemisphere's values for ΔS and M are approximately 1/3 smaller and 7 times larger respectively, in the Southern than in the Northern Hemisphere. The reduction in γ for the Southern Hemisphere is therefore primarily controlled by the increased mass transport M being greater than the reduction in ΔS within the region.

7. Conclusion

Building upon the analysis of Stommel and Csanady (1980), a simple relation between the ratio of poleward heat transport by the ocean (H_o) and the atmosphere (H_a) and the oceanic T/S curve was derived –eq. (17). The relation was tested succesfully against the control simulation of a coupled climate model and hydrographic observations. In both datasets a dominance of atmospheric heat transport in middle latitudes is found.

The relation (17) offers a new perspective on the mechanisms of poleward heat transport

in the climate system. The ratio H_o/H_a was shown to depend solely on two parameters: the ratio γ of dry static energy to latent heat transport, and the slope μ of the T/S curve drawn by equatorward and poleward moving water masses. Different oceanic and atmospheric processes (eddies, zonally averaged circulations) operate at different values of the parameters μ and γ. For example, it was shown that Southern ocean eddies are associated, at $45°S$, with values of $\mu \simeq 8K/psu$, larger than those of the large scale circulation ($\simeq 1K/psu$, see Fig. 5, grey). Comparison of both hemispheres indicated that these two terms show a partial compensation in (17), helping to keep the ratio H_o/H_a almost symmetric about the equator. More work is required to explain this intriguing compensation.

APPENDIX

Derivation of γ_{sst} - Eq. (21)

To derive equation (21) we limit ourselves to mid-latitudes, where the main mechanism of latent heat transport is through atmospheric eddies,

$$l_v F \approx l_v \int \overline{v'q'} \frac{dP}{g} \tag{A1}$$

At fixed relative humidity RH, greater air temperature T' correspond to an increase in the specific humidity q',

$$q' = (dq_{sat}/dT)\, RH \times T' \tag{A2}$$

where we have rewritten q = RH$\times q_{sat}$, with q$_{sat}$ being equal to the saturation specific humidity. Relative humidity is set to 0.8 which is close to lower tropospheric values (Pierrehumbert, 2002). By multiplying the above equation by v', using our approximation for latent heat transport and our expression for γ in Eq. (11), we can derive a new expression of γ such that

$$\gamma = \frac{c_p}{l_v RH} \left(\frac{dq_{sat}}{dT} \right)^{-1} \tag{A3}$$

This can be developed further by using the Clausius-Clapeyron expression linking humidity changes to temperature changes (Hartmann, 1994)

$$\frac{dq_{sat}}{dT} = \frac{l_v}{RT_s^2} q_{sat}, \tag{A4}$$

where $R = 287 JKg^{-1}K^{-1}$ is the Gas Constant for water vapour and T_s is the surface temperature. By combining the latter expression with $(A3)$, we readily obtain,

$$\gamma_{T_s} = \frac{c_p R}{l_v^2 RH} \frac{T_s^2}{q_{sat}(T_s)} \tag{A5}$$

The latitudinal distribution of γ_{T_s} for both hemispheres can be seen in Fig.5b (dashed lines) in which we have used zonal average values for T_s. The model values i.e. γ_F (solid lines) shows similar values of approximately 2 at middle latitudes $(40^\circ N)$, which is of similar magnitude to NCEP observations of $\gamma \approx 1.4$ (Pierrehumbert, 2002). The increase in magnitude with latitude is due to latent heat transport decreasing at a faster rate as compared to dry static energy, since at colder air temperatures the atmosphere's ability to store moisture is greatly reduced. The agreement between γ_{T_s} and γ_f is good in the Northern Hemisphere but, as was found for the ratio H_o/H_a, poor in the Southern Hemisphere.

List of Figures

REFERENCES

-Bjerknes J., 1964: Atlantic air-sea interaction. Advances in Geophysics, Vol. 10, Academic Press, 182.

-Bryden, H. L., and S. Imawaki, 2001: Ocean heat transport, in Ocean Circulation and Climate, Academic Press.

-Carissimo, B. C., A. H. Oort, and T. H. V. Haar, 1985: Estimating the meridional energy transports in the atmosphere and ocean, J. Phys. Oceanogr., 15, 82-91.

-Cox, P. M., R. A. Betts, C. B. Bunton, R. L. H. Essery, P. R. Rowntree, and J. Smith, 2000: The impact of new land surface physics on the gcm simulation of climate and climate sensitivity, Climate. Dyn., 15, 183-203.

-Czaja A., and J. Marshall, 2006: The partitioning of the poleward heat transport between Atmosphere and Ocean, J. Atm. Sci., 63, 1498-1511.

-Gill, A. E. J., 1982: Atmosphere - Ocean Dynamics, Academic press.

-Gordon C., C. Cooper, C. A. Senior, H. Banks, J. M. Gregory, T. C. Johns, J. F. B. Mitchell, and R. A. Wood, 2000: The simulation of sst, sea ice extents and ocean heat transports in a version of the hadley centre coupled model without flux adjustments, Climate. Dyn., 16, 147-168.

-Haar T. H. V., and A. H. Oort, 1973: New estimate of annual poleward energy transport by northern hemisphere oceans, J. Phys. Oceanog., 3, 169-172.

Hartmann, D. L., 1994: Global Physical Climatology, Academic Press

-Held I. M., and B. J. Soden, 2000: Water vapor feedback and global warming, Annu. Rev. Energy Environ., 25, 441-475.

-Held. I. M., 2001: The partitioning of the poleward energy transport between the tropical ocean and atmosphere, J. Atmos. Sci., 58, 943-948.

-Held, I. M., and B. J. Soden, 2006: Robust responses of the hydrological cycle to global warming, J. Clim., 19, 5686-5699.

-Houghton H. G., 1954: On the annual heat balance of the northern hemisphere, J. Meteor., 11, 1-9.

-Jayne S. R., and J. Marotzke, 2002: The oceanic eddy heat transport, J. Phys. Oceanogr., 32, 3328-3344.

-Keith D. W., 1995: Meridional energy transport: uncertainty in zonal means, Tellus, 47A, 30-44.

-Lorenz D. J., and E. T. DeWeaver, 2007: The response of the extratropical hydrological cycle to global warming, J. Climate, 20, 3470-3484.

-Meijers, A. J.,N. L. Bindoff and J. L. Roberts, 2007: On the total, mean, and eddy heat and freshwater transports in the southern hemisphere of a 1/8° x 1/8° global ocean model, J. Phys. Oceanogr., 37, 277-295.

-Neelin J. D., and I. M. Held, 1987: Modelling tropical convergence based on the moist static energy budget, Monthly Weather Rev., 115, 3-12.

-Nilsson J., and H. Kornich, 2008: A conceptual model of the surface salinity distribution in the oceanic hadley cell, J. Climate, 21, 6586-6598.

-Pardaens A. K., H. T. Banks, J. M. Gregory, and P. R. Rowntree, 2003: Freshwater transports in hadcm3, Climate Dynamics, 21, 177-195.

-Peixoto J. P., and A. H. Oort, 1992: Physics of Climate, AIP Press.

-Pierrehumbert, R. T., 2002: The hydrological cycle in deep time climate problems, Nature, 419, 191-198.

-Pope V. D., M. L. Gallani, P. R. Rowntree, and R. A. Stratton, 2000: The impact of new physical parametrizations in the hadley centre climate model: HadAM3. Climate Dynamics, 16, 123-146.

-Plumb, R. and J. Mahlman, 1987: The zonally-averaged transport characteristics of the GFDL general circulation/transport model. J. Atmos. Sci. 44, 298327.

-Stommel, H. M., and G. T. Csanady, 1980: A relation between the T-S curve and global heat and atmospheric water transports, J. Geophys. Res., 85(C1), 495501.

-Stone P. H., 1978: Constraints on dynamical transports of energy on a spherical planet, Dyn. Atmos. Oceans, 2, 123-139.

-Stouffer, R.J., A.J. Broccoli, T.L. Delworth, K.W. Dixon, R. Gudgel, I. Held, R. Hemler, T. Knutson, H.C. Lee, M.D. Schwarzkopf, B. Soden, M.J. Spelman, M. Winton, and F. Zeng, 2006: GFDL's CM2 Global Coupled Climate Models. Part IV: Idealized Climate Response. J. Climate. 19, 723740

-Sverdrup H. U., 1957: Oceanography, Springer-Verlag.

-Trenberth K. E., and J. M. Caron, 2001: Estimates of meridional atmosphere and ocean heat transports, J. Climate, 14, 3433-3443.

-Vecchi G. A., and B. J. Soden: Global warming and the weakening of the tropical circulation, J. Climate, 20, 4316-4340.

-White, N,. 1994: Research Summary, cruise FR 10/94. CSIRO Division of Oceanography for Franklin National Facility, 8pp -see http@//whpo.ucsd.edu/data/onetime/southern/s05/index/htm

-Wunsch C., 1999: Where do ocean eddy heat fuxes matter?, J. Geophys. Res., 104(C6), 13, 235-249.

-Wunsch C., 2005: The Total Meridional Heat Flux and Its Oceanic and Atmospheric Partition, J. Climate, 18, 4374-4380

-Wunsch C., and P. Heimbach, 2006: Estimated decadal changes in the north atlantic meridional overturning circulation and heat flux 1993-2004, J. Phys. Oceanogr., 36, 2012-2024.

-Wunsch, C., 2007: The past and future ocean circulation from a contemporary perspective, Geophys. Monograph Series 173, doi:10.1029/173GM06.

List of Figures

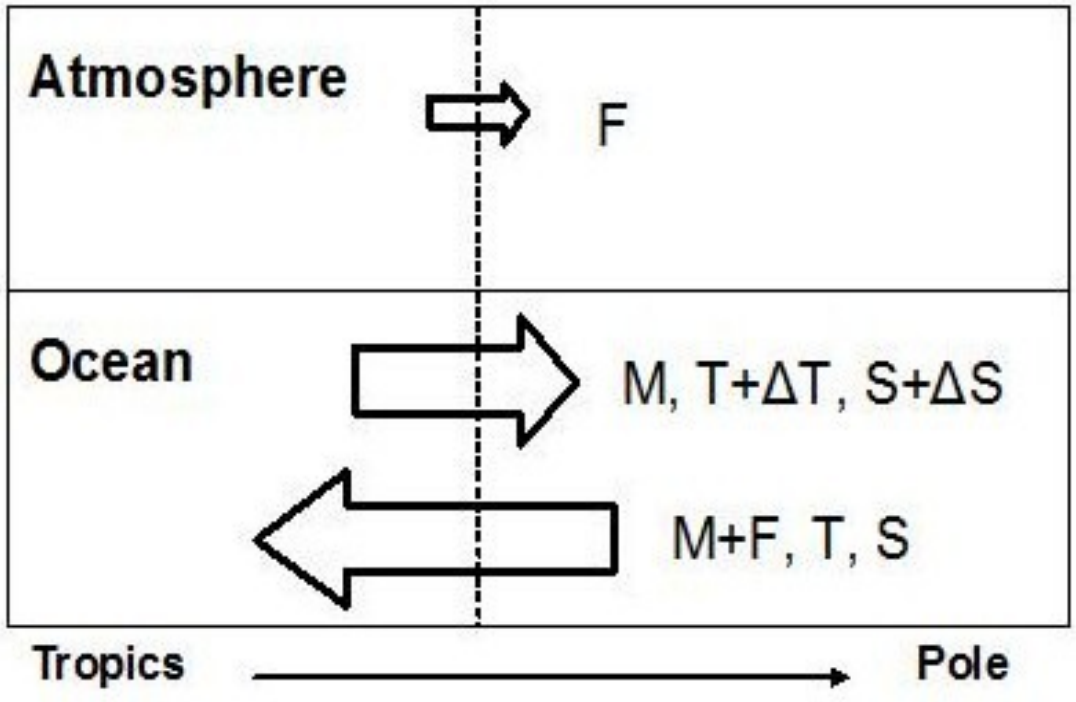

FIG. 1. Stommel and Csanady's analysis of the oceanic heat and freshwater budgets. The poleward atmospheric and oceanic transport of water across a given latitude (indicated by the dashed line) is denoted by F and M, respectively. A net amount F of freshwater must return equatorward in the ocean in steady state, as indicated by the difference between the northward flowing water masses (salinity $S+\Delta S$,temperature $T+\Delta T$) and the equatorward flowing water masses (salinity S, temperature T). Note that the poleward flowing oceanic water masses have been placed arbitrarily above the equatorward flowing ones for clarity of drawing (they do not have to, for instance if horizontal gyres carry the different water masses).

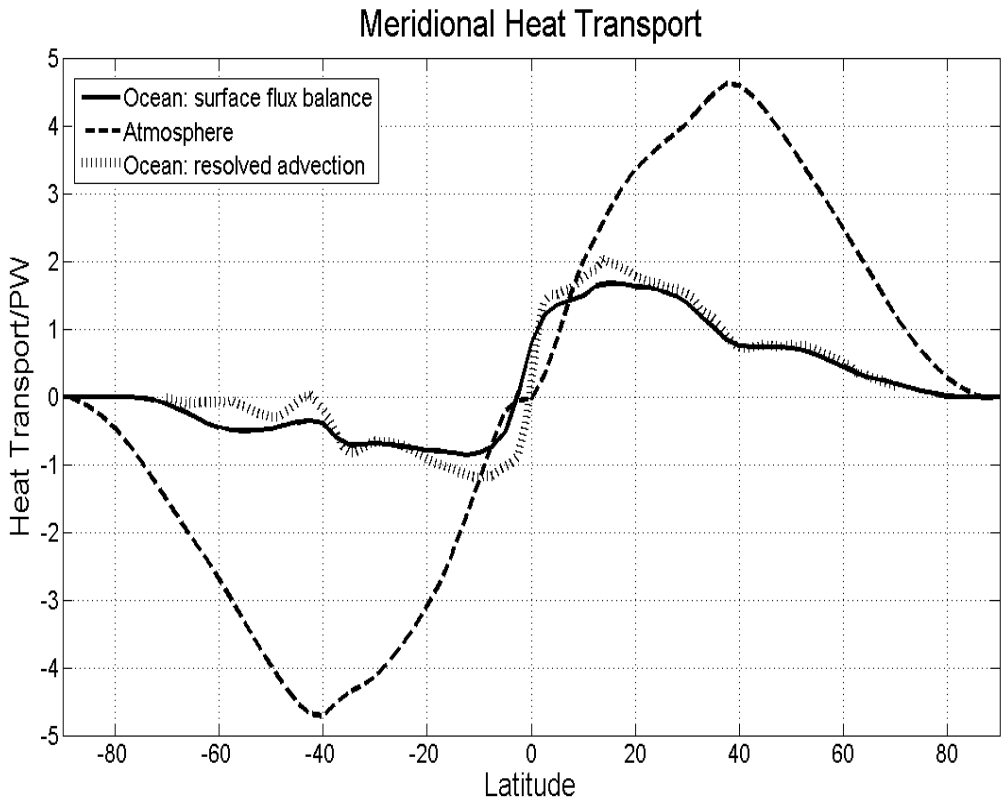

FIG. 2. Meridional Heat Transport computed from HadCM3 decomposed into components for the atmosphere (dashed), the ocean computed from surface flux divergence (solid), and the ocean resolved advective term (dotted).

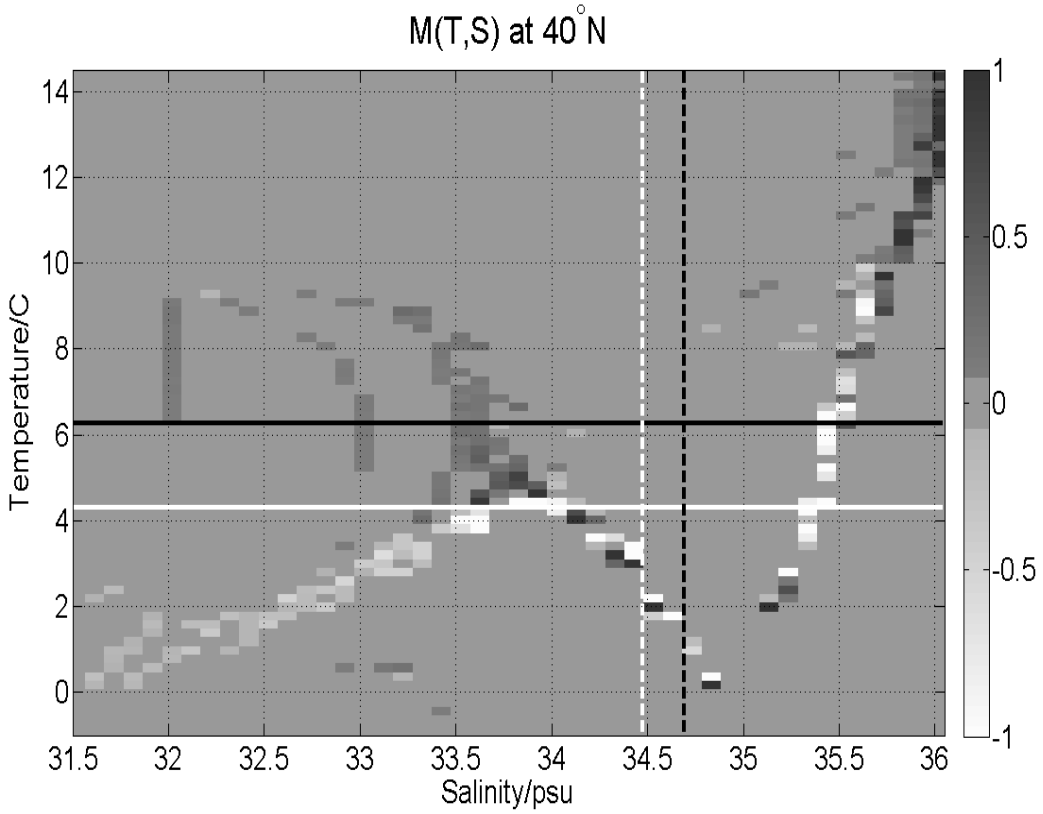

FIG. 3. Plot of Mass Transport M as a function of salinity (x-axis) and temperature (y-axis). Mass weighted values of temperature (salinity) for meridional moving waters are represented by the solid (dashed) lines. Dark (light) shading refers to poleward (equatorward) flowing waters. Values of mass transport are divided by a constant density $\rho_o = 1025 kgm^{-3}$ to have the same units of volume flux measured in Sv.

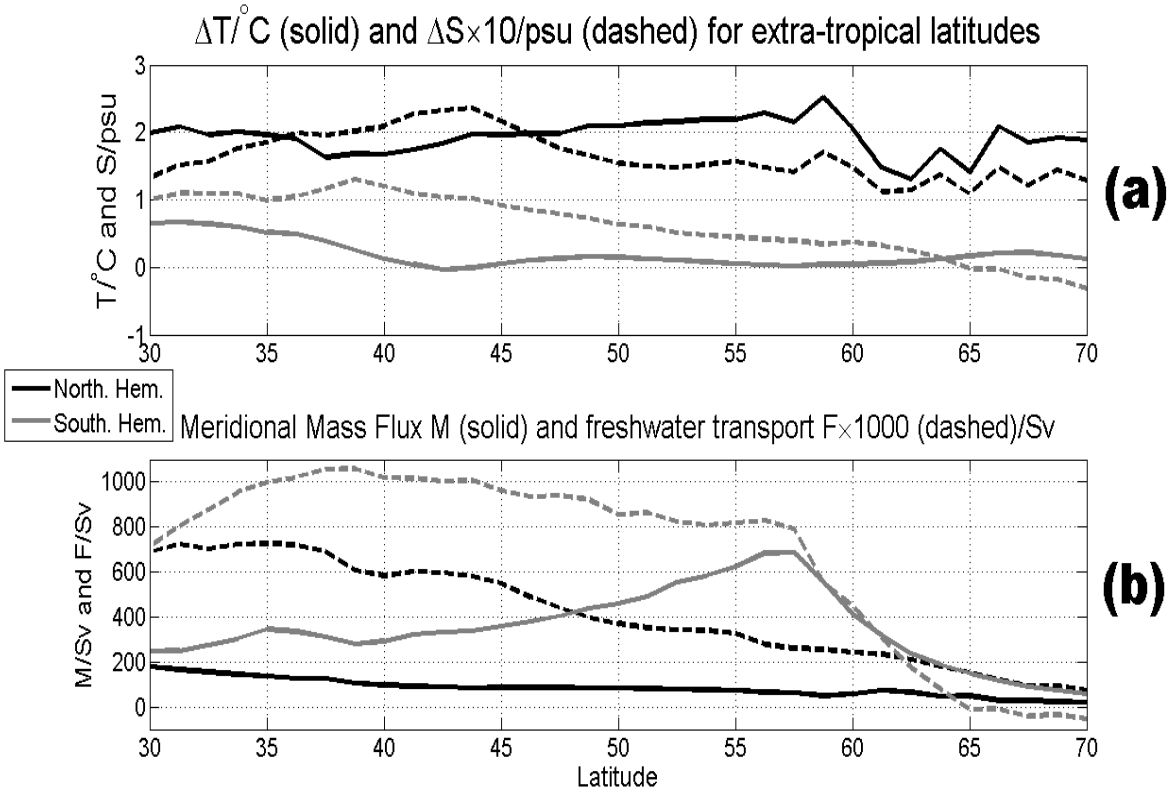

FIG. 4. Distribution of ΔT, ΔS, meridional mass transport M, and freshwater transport F in the atmosphere. Northern (Southern) hemisphere values are represented by black (grey) lines. ΔS (a) is multiplied by factor of 10 to highlight the salinity features, with the southern hemispheric freshwater transport being multiplied by a factor of 1000 for similar reasons. The latitudinal axis for the southern hemisphere plots are reflected such that they overlap that for the northern hemisphere.

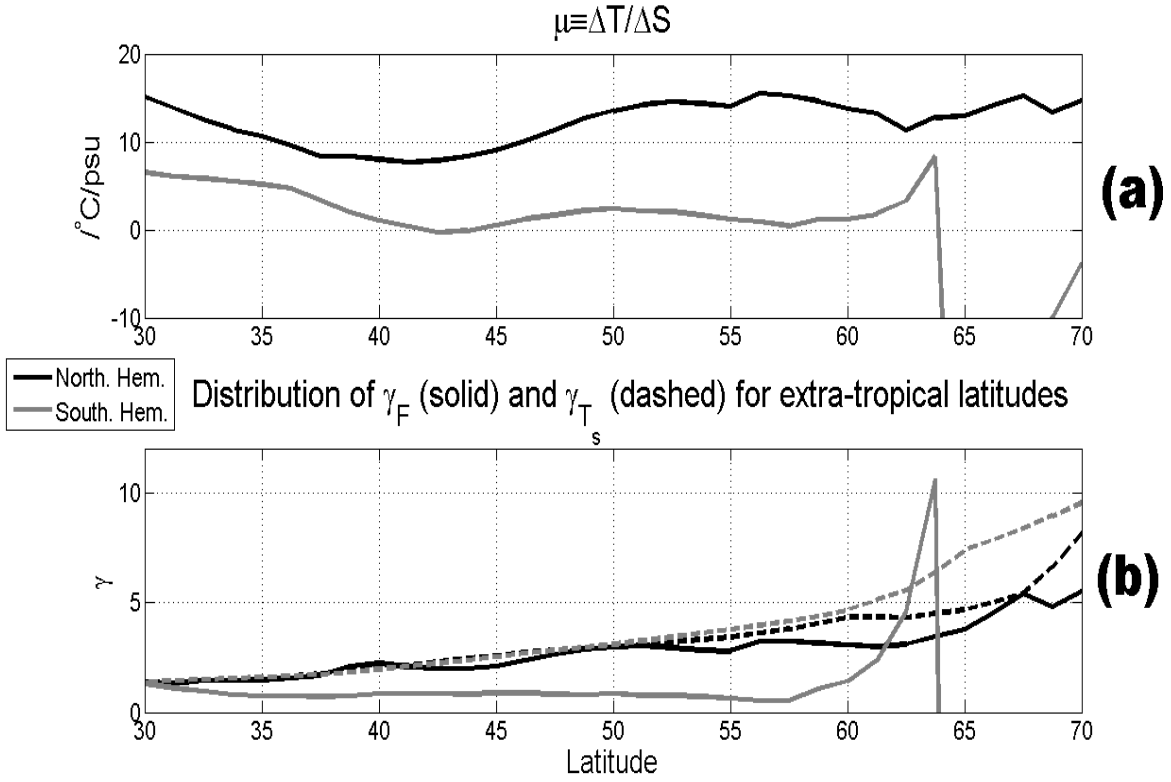

FIG. 5. Distribution of the T/S slope μ (a), and the model observed values for the ratio of dry static energy to latent heat transport in the atmosphere, γ (b). Northern (Southern) hemisphere values are shown in black (grey), with true γ_F (solid) computed from freshwater transports, and predicted γ_{T_s} (dashed) computed from zonally averaged surface temperatures.

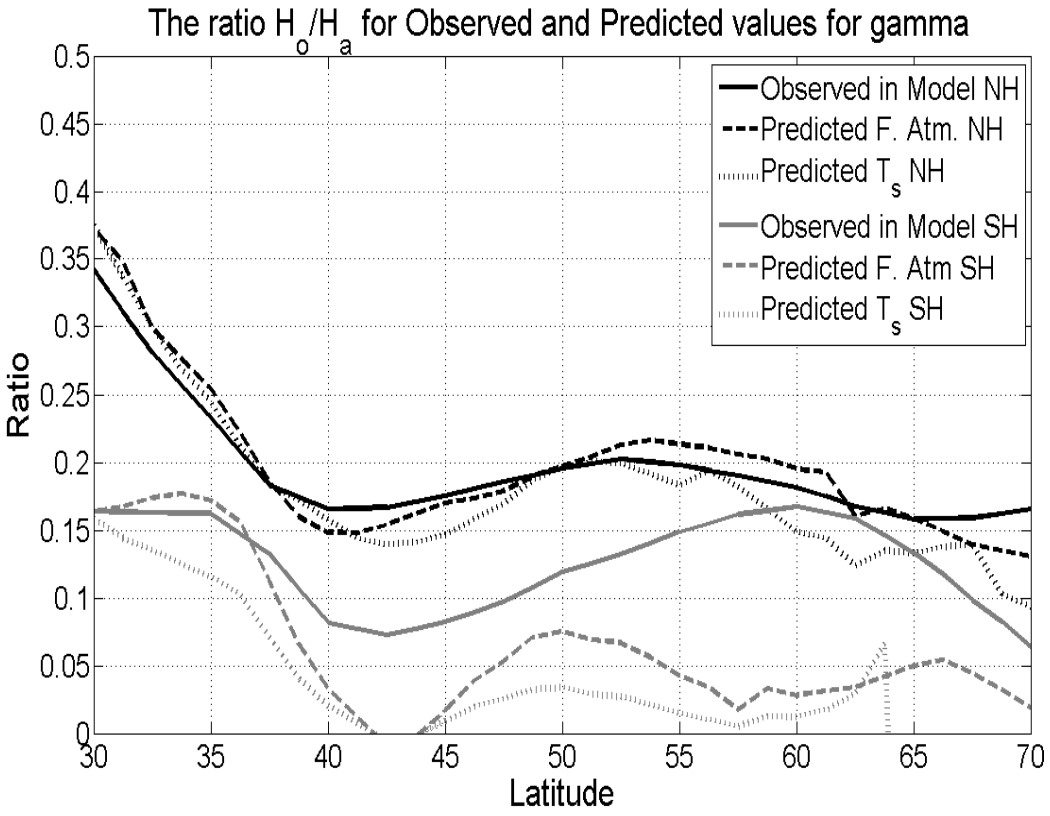

FIG. 6. The ratio H_o/H_a in HadCM (solid) and predicted from (17) using γ_F (dashed). Plots in black (grey) represent the Northern (Southern) Hemisphere. The dotted lines corresponds to an additional calculation in which $\gamma = \gamma_{T_s}$ is predicted rather than calculated in the model.

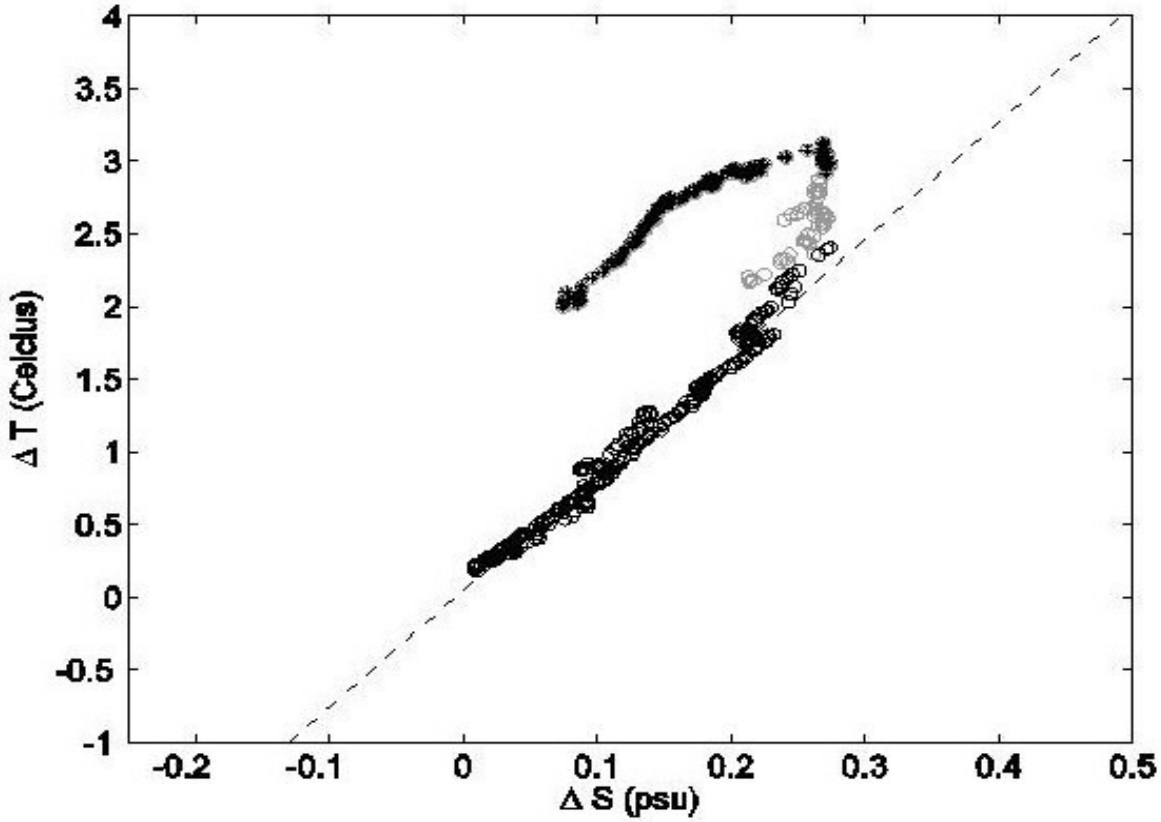

FIG. 7. Meridional salinity (in *psu*) and potential temperature (in degree Celcius) contrasts across $45°S$ as estimated from WOCE section's S05. The dashed line indicates the $8K/psu$ line.

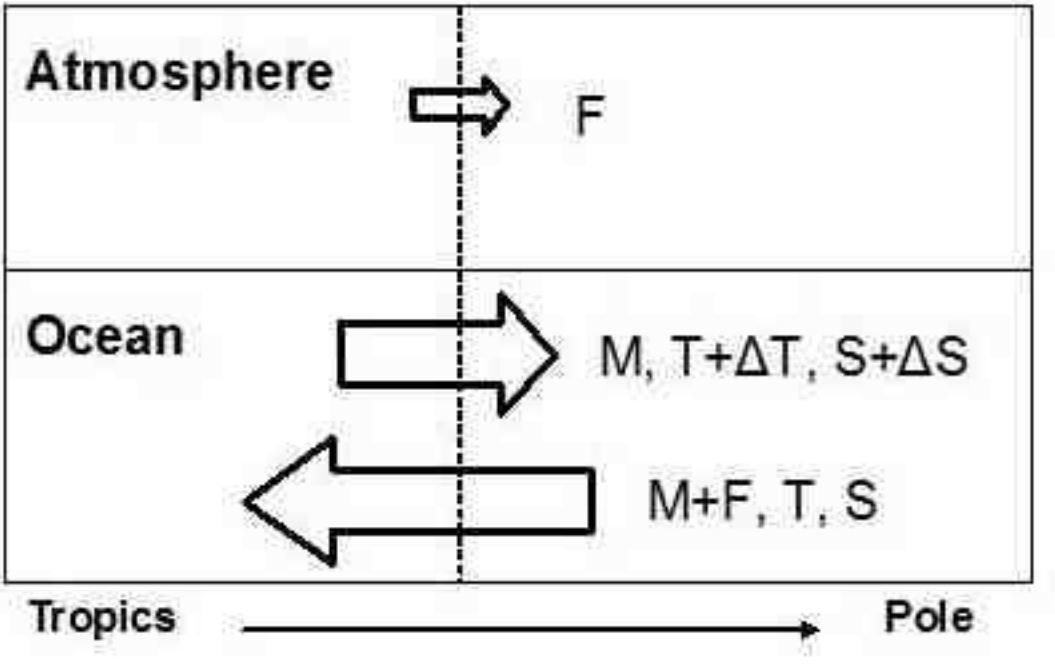
Atmosphere
F
Ocean
M, T+ΔT, S+ΔS
M+F, T, S
Tropics
Pole

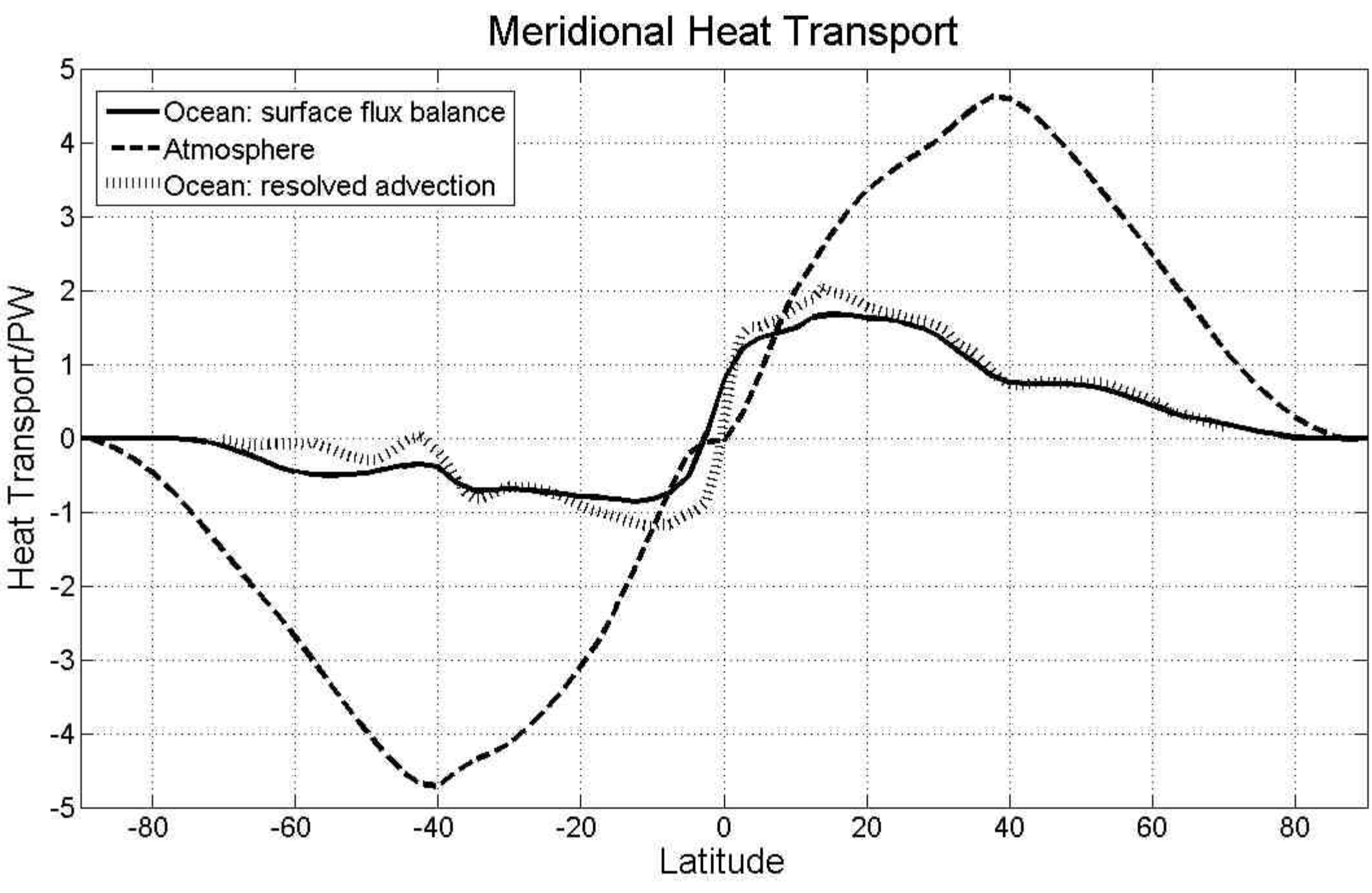
Meridional Heat Transport
Ocean: surface flux balance
Atmosphere
Ocean: resolved advection
Heat Transport/PW
Latitude
5
4
3
2
1
0
-1
-2
-3
-4
-5
-80
-60
-40
-20
0
20
40
60
80

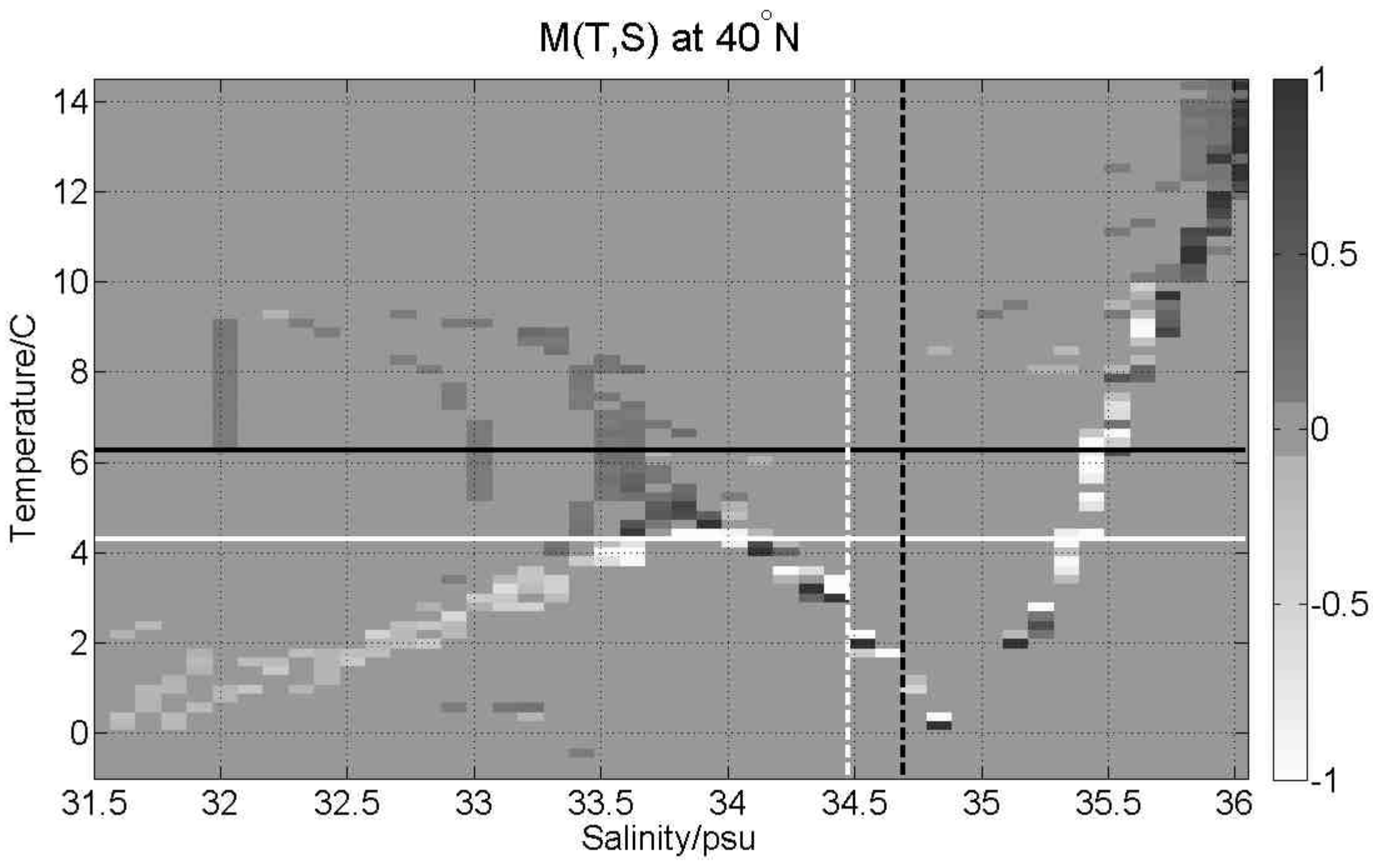
M(T,S) at 40°N
Temperature/C
Salinity/psu
14
12
10
8
6
4
2
0
31.5
32
32.5
33
33.5
34
34.5
35
35.5
36
1
0.5
0
-0.5
-1

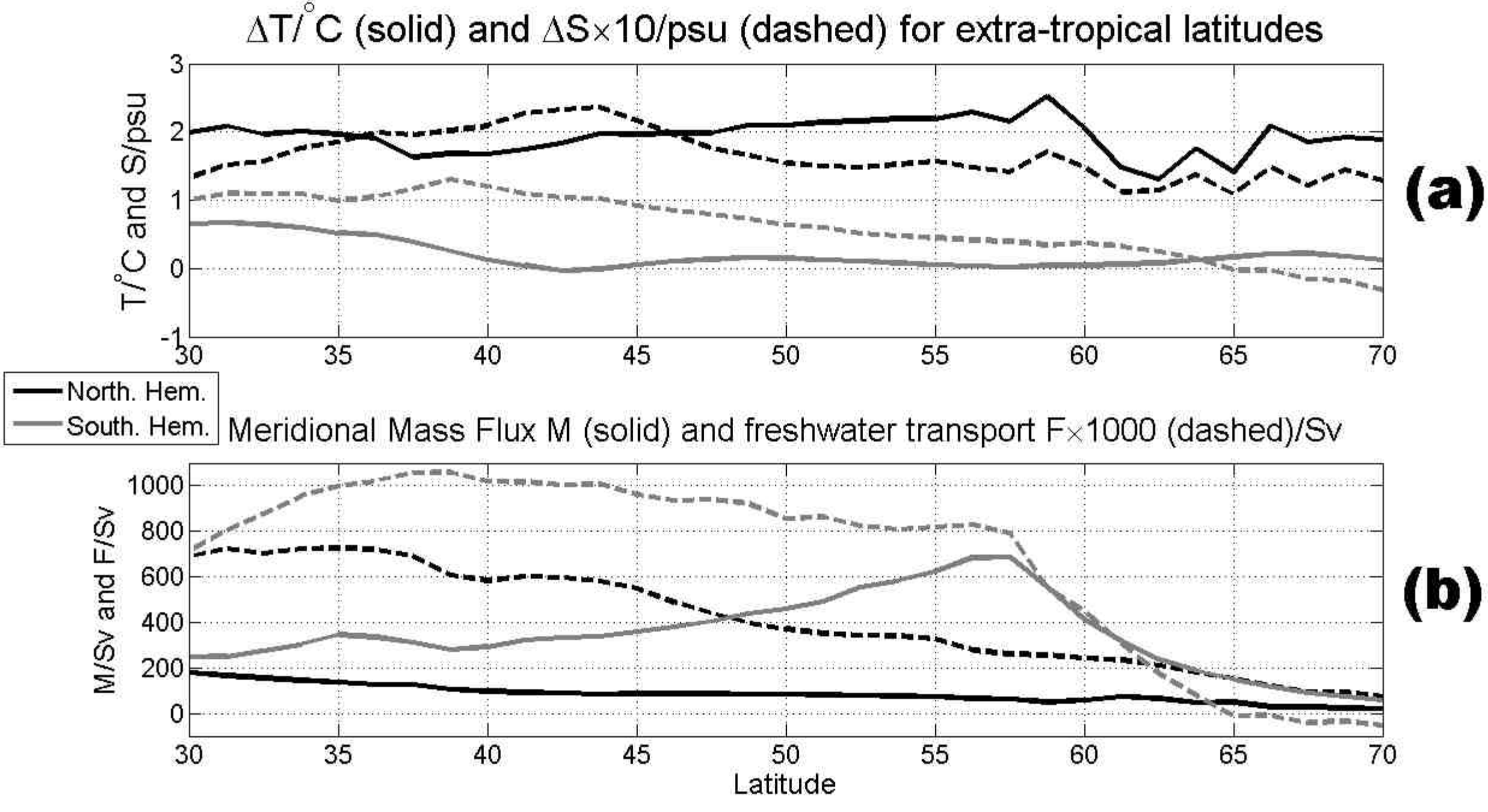
ΔT/°C (solid) and ΔS×10/psu (dashed) for extra-tropical latitudes
T/°C and S/psu
3
2
1
0
-1
30
35
40
45
50
55
60
65
70
(a)
North. Hem.
South. Hem.
Meridional Mass Flux M (solid) and freshwater transport F×1000 (dashed)/Sv
M/Sv and F/Sv
1000
800
600
400
200
0
Latitude
(b)

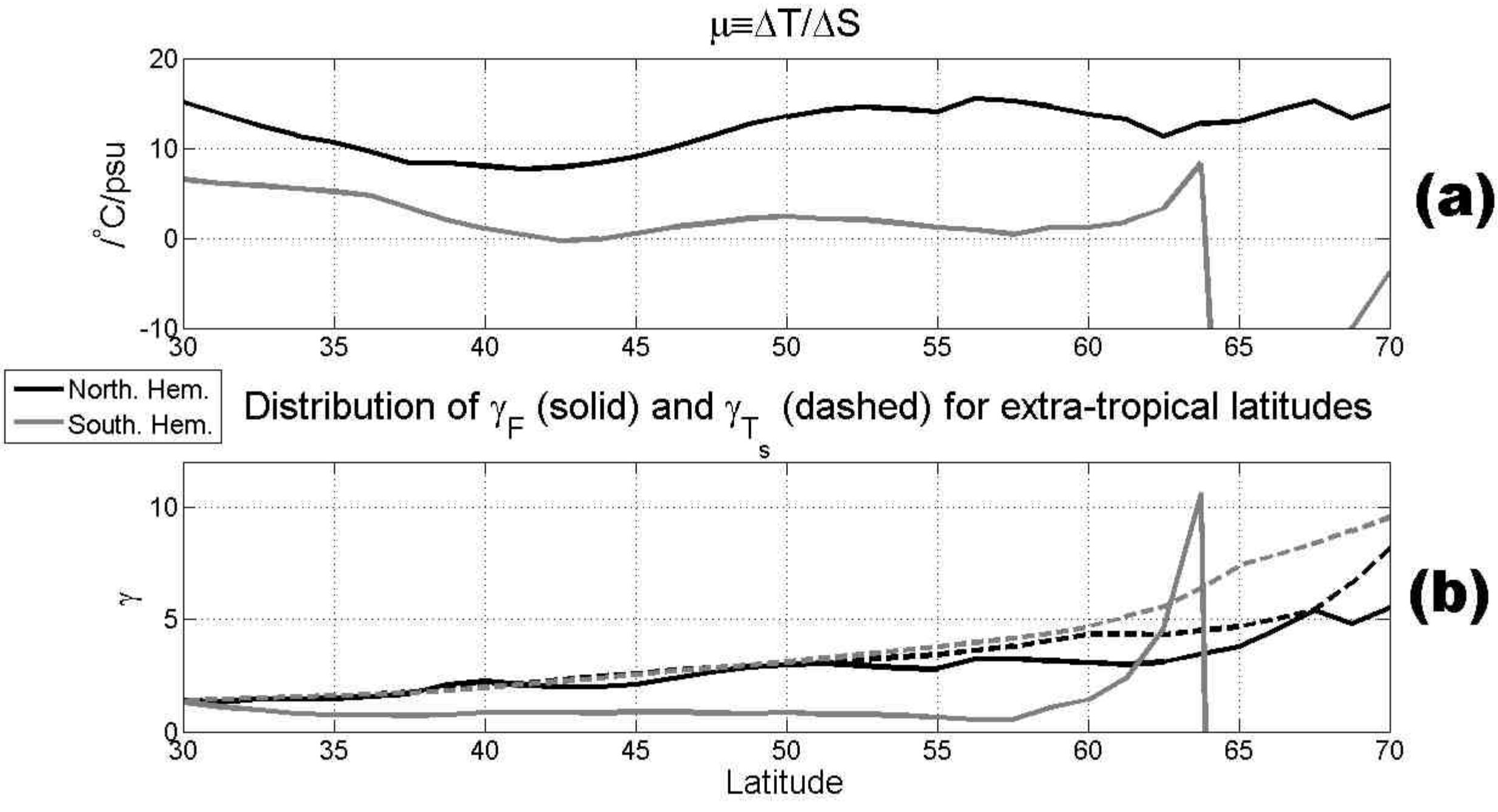
μ≡ΔT/ΔS
20
10
0
-10
°C/psu
30
35
40
45
50
55
60
65
70
(a)
North. Hem.
South. Hem.
Distribution of γF (solid) and γTs (dashed) for extra-tropical latitudes
10
5
0
γ
(b)
Latitude

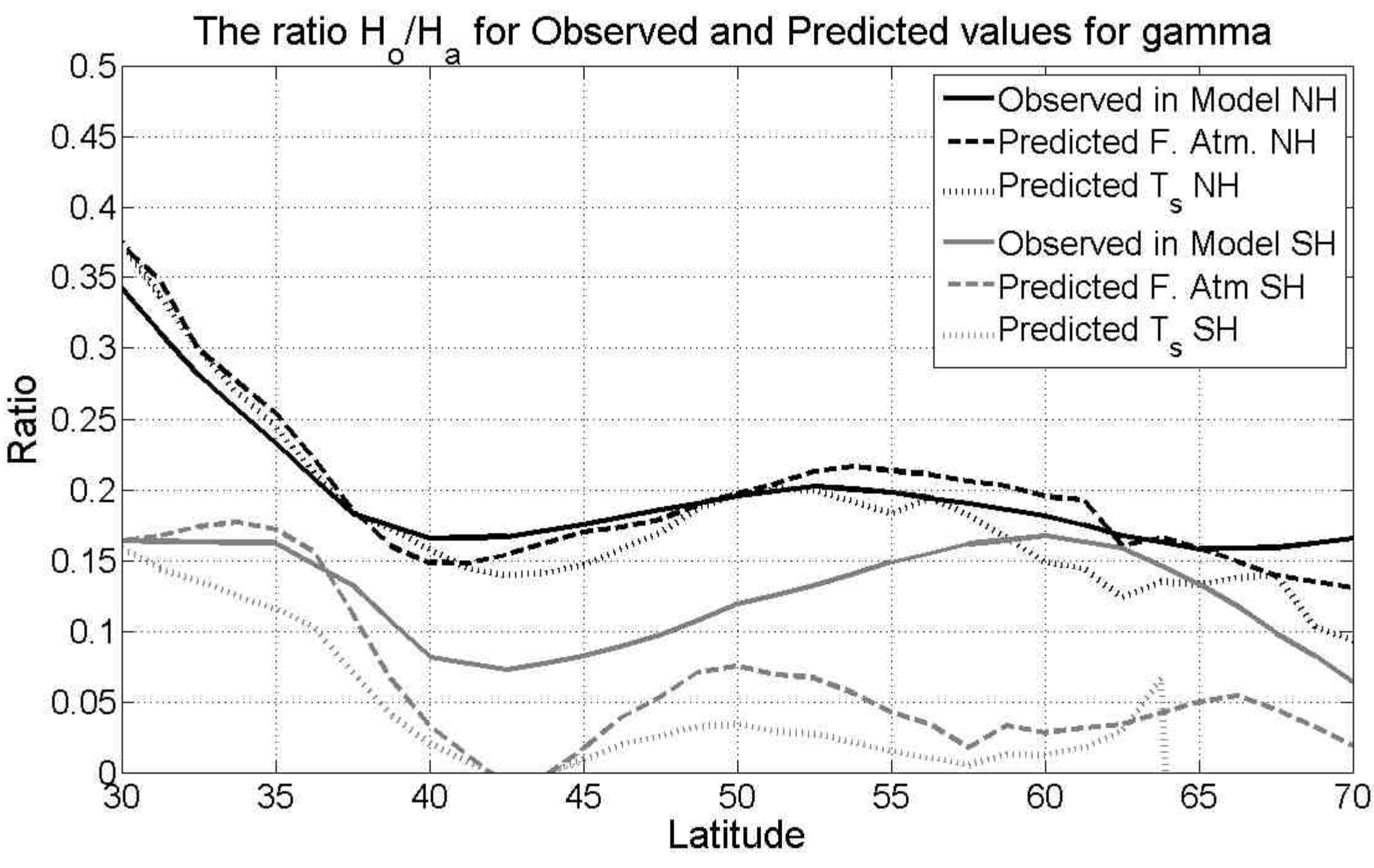
The ratio H_o/H_a for Observed and Predicted values for gamma
Observed in Model NH
Predicted F. Atm. NH
Predicted T_s NH
Observed in Model SH
Predicted F. Atm SH
Predicted T_s SH
Ratio
Latitude
0.5
0.45
0.4
0.35
0.3
0.25
0.2
0.15
0.1
0.05
0
30
35
40
45
50
55
60
65
70

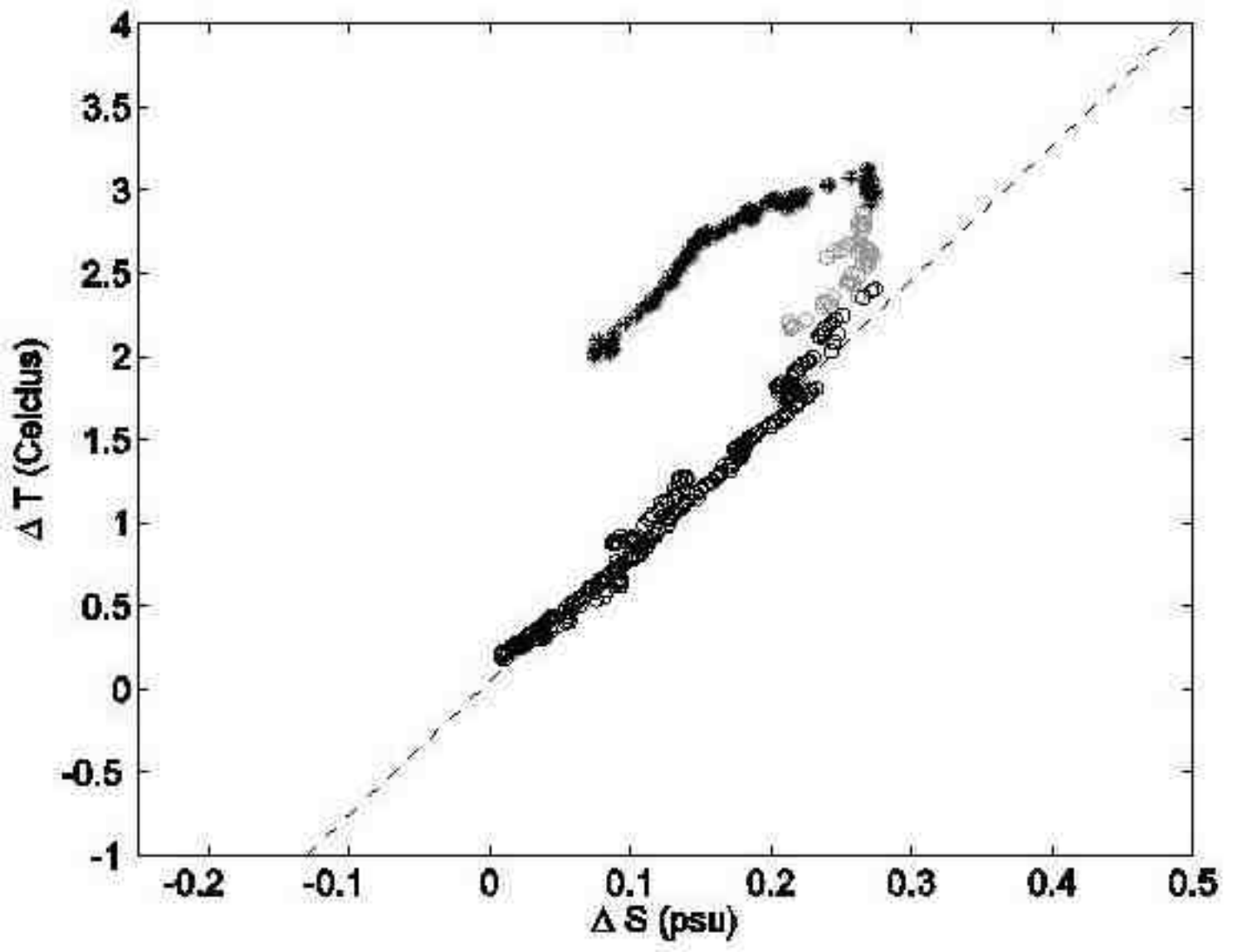
4
3.5
3
2.5
2
1.5
1
0.5
0
-0.5
-1
ΔT (Celcius)
-0.2
-0.1
0
0.1
0.2
0.3
0.4
0.5
ΔS (psu)